Proc. Natl. Acad. Sci. USA
Vol. 93, pp. 13182–13187, November 1996
Medical Sciences

NADPH-oxidase and a hydrogen peroxide-sensitive K^+ channel may function as an oxygen sensor complex in airway chemoreceptors and small cell lung carcinoma cell lines

(pulmonary neuroepithelial bodies/oxygen sensing/reactive oxygen intermediates/nonisotopic *in situ* hybridization)

DASHOU WANG*, CHARLOTTE YOUNGSON*, VERONICA WONG*, HERMAN YEGER*, MARY C. DINAUER†, ELEAZAR VEGA-SAENZ DE MIERA‡, BERNARDO RUDY‡, AND ERNEST CUTZ*§

*Department of Pathology, The Research Institute, The Hospital for Sick Children and University of Toronto, 555 University Avenue, Toronto, ON, Canada M5G 1X8; †Department of Pediatrics (Hematology/Oncology), Herman B. Wells Center for Pediatric Research, James Whitcomb Riley Hospital for Children, 702 Barnhill Drive, Indiana University Medical Center, Indianapolis, IN 46202; and ‡Department of Physiology and Neuroscience, New York University Medical Center, School of Medicine, 550 First Avenue, New York, NY 10016

Communicated by Ewald R. Weibel, Universität Bern, Bern, Switzerland, August 14, 1996 (received for review January 25, 1996)

ABSTRACT **Pulmonary neuroepithelial bodies (NEB) are widely distributed throughout the airway mucosa of human and animal lungs. Based on the observation that NEB cells have a candidate oxygen sensor enzyme complex (NADPH oxidase) and an oxygen-sensitive K^+ current, it has been suggested that NEB may function as airway chemoreceptors. Here we report that mRNAs for both the hydrogen peroxide sensitive voltage gated potassium channel subunit (KH_2O_2) KV3.3a and membrane components of NADPH oxidase ($gp91^{phox}$ and $p22^{phox}$) are coexpressed in the NEB cells of fetal rabbit and neonatal human lungs. Using a microfluorometry and dihydrorhodamine 123 as a probe to assess H_2O_2 generation, NEB cells exhibited oxidase activity under basal conditions. The oxidase in NEB cells was significantly stimulated by exposure to phorbol esther (0.1 μM) and inhibited by diphenyliodonium (5 μM). Studies using whole-cell voltage clamp showed that the K^+ current of cultured fetal rabbit NEB cells exhibited inactivating properties similar to KV3.3a transcripts expressed in *Xenopus* oocyte model. Exposure of NEB cells to hydrogen peroxide (H_2O_2, the dismuted by-product of the oxidase) under normoxia resulted in an increase of the outward K^+ current indicating that H_2O_2 could be the transmitter modulating the O_2-sensitive K^+ channel. Expressed mRNAs or orresponding protein products for the NADPH oxidase membrane cytochrome b as well as mRNA encoding KV3.3a were identified in small cell lung carcinoma cell lines. The studies presented here provide strong evidence for an oxidase-O_2 sensitive potassium channel molecular complex operating as an O_2 sensor in NEB cells, which function as chemoreceptors in airways and in NEB related tumors. Such a complex may represent an evolutionary conserved biochemical link for a membrane bound O_2-signaling mechanism proposed for other cells and life forms.**

Pulmonary neuroepithelial bodies (NEB) are innervated clusters of amine and peptide containing cells located within the airway mucosa, particularly at airway bifurcations (1, 2). Although the physiologic function of NEB is presently unknown, Lauweryns and Cokeleare (1), over 25 years ago, proposed that their role to be that of hypoxia sensitive airway sensors.

The notion that NEB represent airway chemoreceptors was strengthened recently by the demonstration that they transduce a hypoxic stimulus via an oxygen sensing mechanism (3) similar, if not identical, to that of arterial chemoreceptors, carotid bodies (4, 5). Using a whole-cell patch clamp technique we have shown that NEB cells isolated from fetal rabbit lungs exhibit membrane properties of excitable cells since they possess voltage activated K^+, Na^+, and Ca^{2+} currents (3). Upon exposure to hypoxia (pO_2 25–30 mmHg) there was reversible reduction in K^+ current without effects on Na^+ or Ca^{2+} currents. By immunohistochemistry using specific antibody against $gp91^{phox}$ of the phagocyte NADPH oxidase, we have localized this glycoprotein to the NEB cell membrane. In subsequent immunohistochemical studies other components of the oxidase ($p22^{phox}$, $p47^{phox}$, $p67^{phox}$, and Rac 2) were also shown to be present in NEB cells of rabbit fetal lung as well as in glomus cells of rat carotid bodies (6).

The above studies have provided strong evidence for the presence in NEB cells of an O_2 sensing mechanism consisting of an O_2 sensor protein complex (NADPH oxidase) coupled to O_2 sensitive K^+ channel as proposed by Lopez-Barneo *et al.* (4, 5). In their "membrane model," hypoxia affects the function of the oxidase via a decrease in the availability of substrate (O_2) resulting in reduced production of O_2 reactive intermediates including H_2O_2, which is likely used as the second messenger molecule to interact with O_2-sensitive K^+ channel. Closure of the O_2 sensitive K^+ channel in turn initiates depolarization of NEB cell membrane leading to opening of voltage sensitive Ca^{2+} channels. The Ca^{2+} influx could trigger the release of neurotransmitters or effect spike duration and/or frequency. Experimental data for hypoxia induced release of serotonin (5-HT; 5-hydroxytryptamine) from NEB cells has, in fact, been obtained both *in vivo* (7) and *in vitro* (8).

The candidate for the O_2 sensor, the NADPH oxidase, is a multisubunit complex that generates superoxide (O_2^-) in the one-electron reduction of O_2 using electrons supplied by NADPH (9–11). The NADPH oxidase is expressed at high levels in neutrophils and macrophages, where superoxide is the precursor to hydrogen peroxide and other reactive oxidants that are used to kill bacteria and fungi (9). The oxidase consists of two membrane proteins ($gp91^{phox}$ and $p22^{phox}$) that together form a b-type cytochrome and two cystolic peptides ($p47^{phox}$ and $p67^{phox}$) (10). A cytosolic small GTPase, Rac, also appears to be required for oxidase activity (11). In neutrophils, the oxidase is activated by assembly of cytosolic with membrane components (11, 12). Heritable defects of either $gp91^{phox}$, $p22^{phox}$, $p47^{phox}$, or $p67^{phox}$ are the basis of chronic granulomatous disease, a disorder of white cell function characterized by recurrent, severe bacterial and fungal infections (11, 12). The genes encoding the different NADPH oxidase components have been cloned and respective cDNA probes generated, thus allowing studies on the expression and localization of different mRNA transcripts in cells and tissues (11).

The publication costs of this article were defrayed in part by page charge payment. This article must therefore be hereby marked "*advertisement*" in accordance with 18 U.S.C. §1734 solely to indicate this fact.

Abbreviations: NEB, neuroepithelial body(ies); KV, K^+ channels; SCLC, small cell lung carcinoma; NISH, nonisotopic *in situ* hybridization; DHR, dihydrorhodamine; DPI, diphenyline iodonium; PMA, phorbol 12-myristate 13-acetate; 5-HT, 5-hydroxytryptamine or serotonin.

§To whom reprint requests should be addressed.

The evidence for H_2O_2 modulation of K^+ channels (O_2-sensitive K^+ channel) is derived from studies of cloned voltage activated K^+ channels (KV) previously referred to as Shaker family of K^+ channels (13). Out of several mRNA transcripts expressed in *Xenopus* oocyte system only three (KV3.3, KV3.4, and KV1.4) have shown inhibition of K^+ channel inactivation upon external application of H_2O_2 (13). Initial studies on tissue and cell distribution of these H_2O_2 sensitive K^+ channel transcripts showed localization in the brain, lung and a small amount in the kidneys (14).

In the present study, we have used nonisotopic *in situ* hybridization (NISH) and Northern blot analysis to localize and identify mRNAs encoding the different components of NADPH oxidase and H_2O_2-sensitive K^+ channel (KV3.3a) in NEB of rabbit and human lung. Molecular probes for different components of NADPH oxidase and KV3.3a were also used to screen small cell lung carcinoma (SCLC) cell lines phenotypically related to NEB in normal lung. The expression of oxidase components in SCLC cell lines at protein level was analyzed by immunohistochemistry. We also used whole-cell patch clamp technique to further characterize inactivating properties of the native O_2 sensitive K^+ channel in NEB cells and the effects of H_2O_2 on this K^+ channel function. Additional evidence for a functioning oxidase in NEB cells is provided by studies using microflourometry with dihydrorhodamine (DHR) 123 as a probe for H_2O_2 generation.

MATERIALS AND METHODS

Tissues and RNA Preparation. Lung tissue samples were obtained from 26-day gestation fetal rabbits. The human lung samples were obtained at autopsy less than 10 hr after death from a newborn infant who died of cerebral aneurysm. The lung tissues were fixed in 10% buffered formalin and embedded in paraffin and 5-μm sections placed on to sialinated slides. Snap frozen lung tissues from rabbit fetuses and autopsy sample of neonatal human lung were used for Northern blot analysis. Total RNAs were extracted by the method of Chomczynski (15). Human mononuclear RNA was prepared as described (16).

Cell Cultures. The SCLC cell lines NCI-H69, NCI-H128, and NCI-H146 were obtained from American Type Culture Collection; NCI-H727, a carcinoid line, was a gift from Adi Gazdar (National Cancer Institute, Bethesda, MD); NCI-H345 small cell carcinoma cell line, a high expressor of bombesin receptor, was a gift from Frank Cuttitta (National Cancer Institute, Rockville, MD); and H69V, an adherent version of the parental line NCI-H69, was a gift from Ian Freshney, (University of Glasgow). The cell lines were maintained in culture media and conditions as reported (17).

The Preparation of cRNA Probes for NADPH Oxidase and KH_2O_2 Channel. The full-length cDNAs for human NADPH oxidase gp91^{phox} and p22^{phox} were cloned in to vector Bluescript KS$^+$ and pGEM9 respectively (16). gp91^{phox} was linearized with *Bam*HI and p22^{phox} with *Sst*I and transcribed with RNA polymerase T3 and SP6 to produce gp91^{phox} and p22^{phox} antisense RNA probes respectively. The rat KH_2O_2 Channel subunit KV3.3a (18) cRNA probe was generated from ≈1-kb cDNA (*Nco*I/*Eco*RI cloned in Bluescript KS$^+$) encoding the 3′ region of the rat KH_2O_2 channel subunit KV3.3a. KV3.3a was linearized with *Nco*I and transcribed with RNA polymerase T7 to produce KV3.3a antisense RNA probe. The digoxigenin-labeled cRNA probes were prepared as described (19).

NISH. *In situ* hybridization was performed with digoxigenin-labeled antisense and sense RNA probes as previously described (19). Briefly, formalin-fixed paraffin embedded sections of rabbit fetal lung (26 days gestation) and human newborn lung were dewaxed and treated with protease VIII to unmask mRNA signal (19). The tumor cell lines grown on Lab-Tech culture slides were fixed in 4% buffered paraformaldehyde for 1 min, rinsed and dehydrated in gradient ethnol before processing for NISH. Proteinase treatment was not required. The protocol for single NISH using DIG-labeled cRNA probes for human gp91^{phox} and p22^{phox} or rat KV3.3a was similar to that described previously (19). Detection of signal was achieved with Dig Nucleic Acid detection kit (Boehringer Mannheim) giving a dark purple color. In some experiments, lung sections were first processed for immunohistochemistry to identify NEB (see below), followed by NISH.

Northern Blot Analysis. Total RNAs were subjected to electrophoresis through 0.8% formaldehyde agarose gel and transferred to Nytran (Schleicher & Schuell) membrane by standard methods (20). The membranes were hybridized with ^{32}P-labeled human gp91^{phox} and rat KV3.3a subunit antisense RNA probes, respectively. Hybridizations were carried out in a solution of 5× SSC, 5 mM NaPO4 (pH 6.5), 0.1% SDS, 1 mM EDTA, 0.05% BSA, 0.05% Ficoll, 0.05% polyvinylpyrrolidone, and 200 μg/ml denatured salmon sperm DNA for 18 hr at 60°C. Membranes were washed at room temperature twice for 15 min each time in 2× SSC/0.2% SDS followed by 2 × 30 min wash in 0.2× SSC/0.1% SDS and exposed for seven days at −70°C to Kodak X-Omat film with an intensifying screen, with the exception of total mononuclear cell RNA, which was exposed for only 18 hr.

Immunohistochemistry. To cross-identify the cells expressing mRNA signal for NADPH oxidase components and/or KH_2O_2 channel we used immunohistochemistry on the same or adjacent section to that used for NISH. The anti-5-HT mAb (Sera-Lab, Crawley Down, Sussex, U.K.) (for rabbit lung) and antibombesin/gastrin releasing peptide polyclonal antibody (Incstar, Stillwater, MI) (for human lung) were used to localize NEB cells in the lung. We used 1:100 dilution of the anti-5-HT antibody with avidin-biotin complex detection method and 1:500 dilution of the antibombesin antibody with a peroxidase-antiperoxidase complex method to visualize NEB cells as described (2, 21).

For localization of various components of NADPH oxidase in tumor cell lines monoclonal and polyclonal antibodies were used according to methods and procedures reported for NEB cells (6). Tumor cells grown on Lab-Tech culture slides (GIBCO) or frozen sections of cell pellets were fixed in 100% ethanol or in 2% paraformaldehyde and immunostained using indirect immunofluorescence method. The following primary antibodies directed against different components of NADPH oxidase were used; mAb against gp91^{phox} (gift from A. Verhoeven, University of Amsterdam), affinity purified rabbit polyclonal antibody against gp91^{phox}, and rabbit polyclonal antibody against p22^{phox} (gift from J. T. Curnutte, Genentech).

In addition to standard immunofluorescence microscopy, laser confocal microscopy was performed using a Leitz (TCS 4D) confocal microscope with argon Krypton laser (excitation at 488 nm for fluorescein isothiocyantate and 567 nm for rhodamine) and pinhole of 40 μm. Signals were analyzed using Scanware (Leica).

Electrophysiology. Whole cell currents were recorded from primary cultures of rabbit fetal NEB. Cultures of NEB were prepared according to a method previously reported (3). In brief, airway epithelium was dissociated from microdissected bronchial trees using 0.2% collagenase (type IV, Sigma). Epithelial fragments were plated on collagen-coated coverslips and maintained at 37°C in 5% CO_2 for 3–7 days in MEM or F12 medium with supplements (3). In living cell culture, NEB clusters were identified using vital dye neutral red (0.02 mg/ml for 30–40 min at 37°C) which is selectively taken up by NEB cells (3).

Whole cell currents in cultured NEB cells were recorded with an Axopatch IB amplifier (Axon Instruments, Burlingame, CA) and a probe equipped with a IGΩ headstage feedback resistor. Typical external recording solutions contained either 140 mM NaCl, 3 mM KCl, 1 mM $MgCl_2$, 1.5 mM $CaCl_2$, 5 mM glucose, and 10 mM Hepes (solution A), or 140 mM choline chloride, 1.5 mM $CoCl_2$, 3 mM KCl, 1 mM Mg Cl, 5 mM glucose, and 10 mM Hepes (solution B). The pH of both solutions was 7.3.

Fluorescence Assay for H_2O_2 Generation Using DHR 123 as a Probe. For measurement of H_2O_2 production by NEB cells as a reflection of functional activity of the oxidase we used

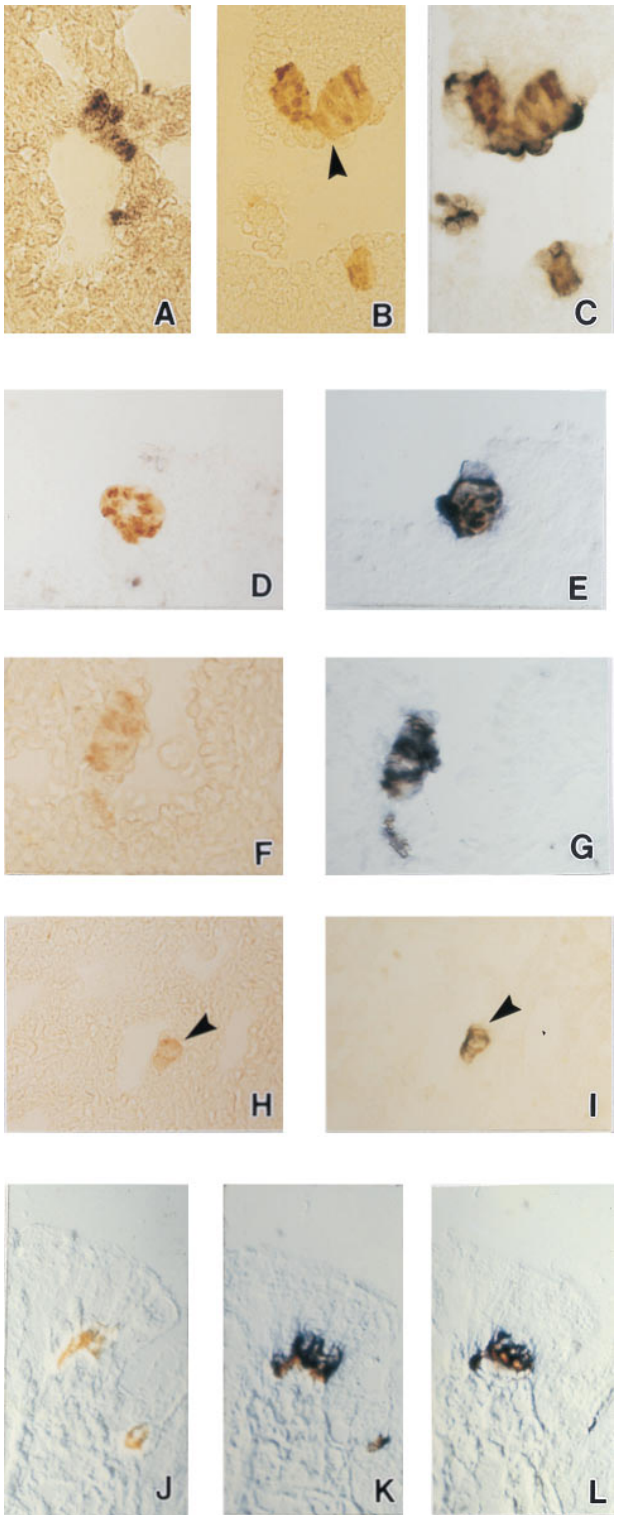

FIG. 1. NISH for gp91^{phox} and p22^{phox} subunits of the NADPH oxidase (O_2-binding protein) components and KH_2O_2 channel KV3.3a in pulmonary NEB of 26 day gestation fetal rabbit lung. (*A*) NISH using the NADPH oxidase subunit gp91^{phox} RNA antisense probe shows specific signal (purple) localized in NEB cells. The section was counter-stained with safranin O. (×400.) (*B*) 5-HT-immunoreactive NEB cells located within airway mucosa at bronchial bifurcation (arrowhead). (×400.) (*C*) NISH on the same section as in *B* using the NADPH oxidase subunit gp91^{phox} RNA antisense probe shows specific mRNA signal (purple blue) localized in the same NEB cells. (×400.) (*D*) Immunostaining for 5-HT (light brown) combined with NISH using the NADPH oxidase subunit gp91^{phox} RNA sense probe (negative control). There is slight focal background staining of lung interstitial cells but no mRNA signal is present in NEB cells indicating specificity of the procedure. (×400.) (*E*) Immunostaining for 5-HT followed by NISH with the NADPH oxidase subunit gp91^{phox} RNA antisense probe on a serial section next to *D*. (×400.) (*F* and *G*) The same tissue and procedures as *B* and *C* using the NADPH oxidase subunit p22^{phox} RNA antisense probe. Strong positive signal for p22^{phox} mRNA (*G*) (purple color) is localized in 5-HT positive NEB cells (brown color) (*F*). Immunostaining for 5-HT followed by (*H*) NISH for KV3.3a using RNA antisense probe (*I*) showing specific mRNA signal (arrowhead) localized in the same 5-HT immunopositive NEB cells. (×250.) Immunostaining of NEB cells for 5-HT in *H* has been purposefully under developed, just enough to allow identification of NEB cells without possible interference of chromogen used in NISH. (*J*) Bombesin immunostaining on formalin fixed paraffin embedded sections of neonatal human lung followed by NISH using the KV3.3a sense RNA probe (negative control). Two bombesin immunoreactive foci (light brown) corresponding to NEB cells within airway epithelium. Absence of mRNA signal indicates specificity of the NISH reaction. (*K*) Bombesin immunostaining followed by NISH with the KV3.3a RNA antisense probe on a serial section next to *J* showing specific expression of the K^+ channel mRNA in NEB cells. (*L*) Bombesin immunostaining followed by NISH with the NADPH subunit gp91^{phox} RNA antisense probe on a serial section next to *K* demonstrating correlation with the K^+ channel mRNA signal in the same NEB cells. (Nomarski interference contrast, ×400.)

reagents and methods similar to those reported by Cross *et al.* (22) for rat carotid body.

DHR 123 (Molecular Probes) was dissolved in dimethyl sulfoxide, aliquoted in dark colored tubes and stored under nitrogen gas at 80°C. The DHR stock solution was diluted in Hepes-buffered physiological saline solution to a final working solution concentration of 10 μM. Phorbol 12-myristate 13-acetate (PMA, Sigma), which stimulates oxidase activity, and diphenylene iodonium (DPI; Toronto Research Chemicals, Downsview, ON, Canada), an inhibitor of oxidase (23), were kept as a 1 mM and 5 mM stock solution in dimethyl sulfoxide and used in a final working dilution of 0.1 μm and 5 μM.

The primary cultures of rabbit fetal lung cells were supravitaly stained with neutral red before each experiment to identify NEB cells in a living state (3). Cell cultures were incubated with DHR working solution either alone or in the presence of PMA or DPI for 20 min at 37°C and rinsed three times in fresh saline solution before viewing. A phase contrast photograph of each microscopic field was taken during the experiment. After completion of experiment the cultures were fixed in 10% neutral buffered formalin and immunostained for 5-HT. In most cases, the cells analyzed were rephotographed to ensure that NEB cells were correctly identified.

The changes in fluorescence intensity of single cells in the presence of DHR were assessed by microfluorometry using a Nikon inverted microscope fitted with a CCD camera with epi-fluorescence illuminator (fluorescein, blue excitation filter, BP 470–490; Nikon). Cells were exposed to UV light for 3 seconds in the presence of a neutral density filter. Fluorescence intensitites were calculated using National Institutes of Health IMAGE software, version 1.57. We obtained signals by tracing around NEB cells of interest as well as representative nonfluorescent background cells.

RESULTS

In rabbit fetal lungs, abundant gp91^{phox} mRNA was specifically localized by NISH to NEB cells (Fig. 1*A*). To confirm the identity of NEB, some sections were first immunostained for 5-HT, marker of NEB (Fig. 1*B*), followed by NISH on the same sections. Colocalization of 5-HT and mRNA signals for gp 91^{phox} was confirmed in the same NEB cells (Fig. 1*C*). To confirm specificity of hybridization reaction, some sections were first immunostained for 5-HT followed by NISH using sense probe for gp91^{phox} (Fig. 1*D*). There was minimal background staining of adjacent lung cells but no signal was detected in NEB cells (Fig. 1*D*). In a serial section adjacent to that of Fig. 1*D*, strong positive signal was localized in NEB cells

when antisense probe for gp91^{phox} was used (Fig. 1*E*). Similar results for NISH were obtained with antisense probes for p22^{phox} (Fig. 1 *F* and *G*). NISH experiments using RNA antisense probes for KV3.3a showed specific localization of mRNA signal in NEB cells (Fig. 1 *H* and *J*).

In sections of human neonatal lung, NEB were identified by positive staining with antibody against bombesin, a peptide expressed in NEB cells of human lung (Fig. 1*K*). When using a sense probe for KV3.3a, no signal was detected in NEB cells (Fig. 1*K*). However, in a serial section probed with antisense, KV3.3a probe, strong signal was localized in NEB cells (Fig. 1*L*). In a serial section next to that of Fig. 1*L*, probed with antisense probe for gp91^{phox} positive signal was localized to the same NEB cluster confirming coexpression of mRNA's encoding gp91^{phox} and KV3.3a in the same NEB cells (Fig. 1*M*). Expression of mRNA for p22^{phox} was also localized with NEB of human lung and was similar to that shown for the rabbit lung (data not shown).

NISH in various SCLC cells lines grown in Lab-Tech chambers showed positive but variable signal for mRNAs encoding NADPH oxidase components (gp91^{phox}, p22^{phox}) as well as the KV3.3a (Fig. 2 *A–C*). Frozen sections of cell pellets of different cell lines immunostained for gp91^{phox} or p22^{phox} and examined under conventional fluorescence microscope, the level of positive immunoreactivity varied between cell lines and with antibodies used (data not shown). Using a confocal microscope providing better resolution, a positive immunolocalization was detected in membranous or submembranous location (Fig. 2*D*). In control sections, where primary antibody was omitted, no signal was detected (not shown). Northern blot analysis of whole lung tissue RNA extracts from rabbit and human lung showed a positive signal for the expected mRNA size for gp91^{phox} and KV3.3a (Fig. 3 *A* and *B*). In SCLC cell lines the intensity of the signal varied between different cell lines. The strongest signal was observed in H727, H69, H345, H146, and H69V respectively and a weak signal in cell line H128.

The presence of an oxidase activity at the cell surface was assessed by incubating cells with nonfluorescent DHR123 and monitoring its conversion into fluorescent rhodamine 123. Thus the assessment of H_2O_2 generation using the fluorescence assay with DHR123 as a probe showed positive fluorescence in NEB cells (Fig. 4*A*), which were further identified by uptake of neutral red and then cross-identified using 5-HT antibody upon completion of the assay. The NEB cells could also be identified by the size of their nuclei which were tightly packed and smaller compared with adjacent nonfluorescent background cells (Fig. 4*A*). Unstimulated NEB cells showed a baseline signal level significantly above that of background cells (Fig. 4*B*). NEB cultures stimulated with PMA showed almost three-fold increase in the fluorescence intensity of the NEB cells with minimal effect on the background cells while incubation with DPI showed a marked decrease in NEB fluorescence intensity (Fig. 4*B*) Taken together these results indicated a dynamic modulation of the oxidase activity in NEB.

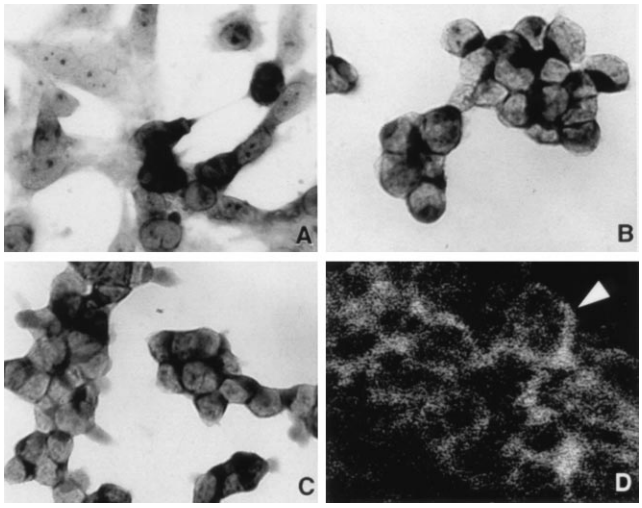

FIG. 2. NISH for gp91^{phox} and KV3.3a with immunohistochemistry for p22^{phox} in SCLC cell lines. (*A*) NISH for gp91^{phox} using RNA antisense probe on H-69V line showing variable expression with strong positive signal in some cells and a weaker or no signal in adjacent tumor cells. (×400.) (*B*) NISH for gp91^{phox} on NCI-H146 cell line showing more uniform cytoplasmic localization of mRNA signal. (*C*) NISH for KV3.3a using antisense RNA probe on NCI-H146 show similar signal distribution as in *B*. (×400.) (*D*) Immunohistochemistry for p22^{phox} on NCI-H146 cell line with membranous or submembranous localization of positive immunoreactivity (arrowhead). (Laser confocal microscopy, fluorescein isothiocyantate-labeled secondary antibody, ×800.)

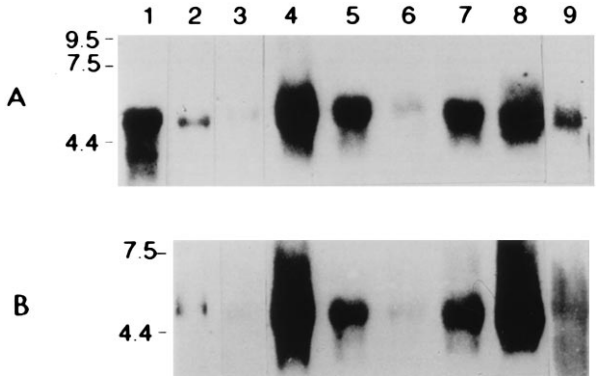

FIG. 3. Northern blot analysis for (*A*) NADPH oxidase subunit gp91^{phox} and (*B*) KH_2O_2 channel subunit (KV3.3a). Lanes: 1, human mononuclear cell RNA extract (control); 2, human lung; 3, fetal rabbit lung; 4–9, SCLC cell lines (H-727, H-345, H-128, H69V, H-69, and H-146). Each lane has 15 μg total RNA and was analyzed by Northern blotting and hybridized with ^{32}P-labeled gp91^{phox} and KV3.3a RNA antisense probe, respectively. In both cases the expected mRNA size of ≈4.7 kb for gp91^{phox} and ≈4.8 kb for KV3.3a was detected as described in previous reports (9, 12).

Patch-clamp experiments substantiated the postulated involvement of an H_2O_2 signal intermediate in chemoreceptor function. Whole cell K^+ current of cultured fetal rabbit NEB cells revealed a slowly inactivating K^+ current (Fig. 5*A*) similar to the one described in *Xenopus* oocytes expressing KV3.3a channels subunit (13). The KV3.3a channel subunit expressed in the model was insensitive to changes in pO_2 but sensitive to H_2O_2. We found that the K^+ current recorded from fetal rabbit NEB cell cultures was increased by exposure to H_2O_2 (Fig. 5 *B* and *C*).

DISCUSSION

Using NISH and Northern blot analysis we demonstrate coexpression of mRNAs encoding the KH_2O_2 channel subunit KV3.3a and the NADPH oxidase cytochrome *b* in NEB of rabbit and human lung. The KH_2O_2 channel probe was generated from ≈1 kb cDNA (*Nco*I/*Eco*RI) encoding the 3′ region of the rat KH_2O_2 channel subunit KV3.3a, which is a region unique for this subunit (14, 18). Previous studies (14) have localized the KV3.3a subunit in rat brain by *in situ* hybridization and Northern blot analysis. Rat lung was one of the few tissues outside the central nervous system where KV3.3a mRNA was expressed (14, 18). We examined expression of KV3.3a along with the oxidase cytochrome b subunits, gp91^{phox} and p22^{phox}, in formalin-fixed paraffin embedded lung tissue sections from late-gestation (26 day) fetal rabbit lungs and neonatal human lungs. Colocalization of mRNAs encoding two of the membrane components of NADPH oxidase and the KH_2O_2 channel was achieved by NISH in combination with immunostaining to confirm NEB cell identity using specific antibodies against well characterized markers for NEB cells (21). Either no signal or weak nonspecific background staining was found in other lung cells. In serial sections, colocalization of message for KH_2O_2 channel subunit KV3.3a and gp91^{phox}

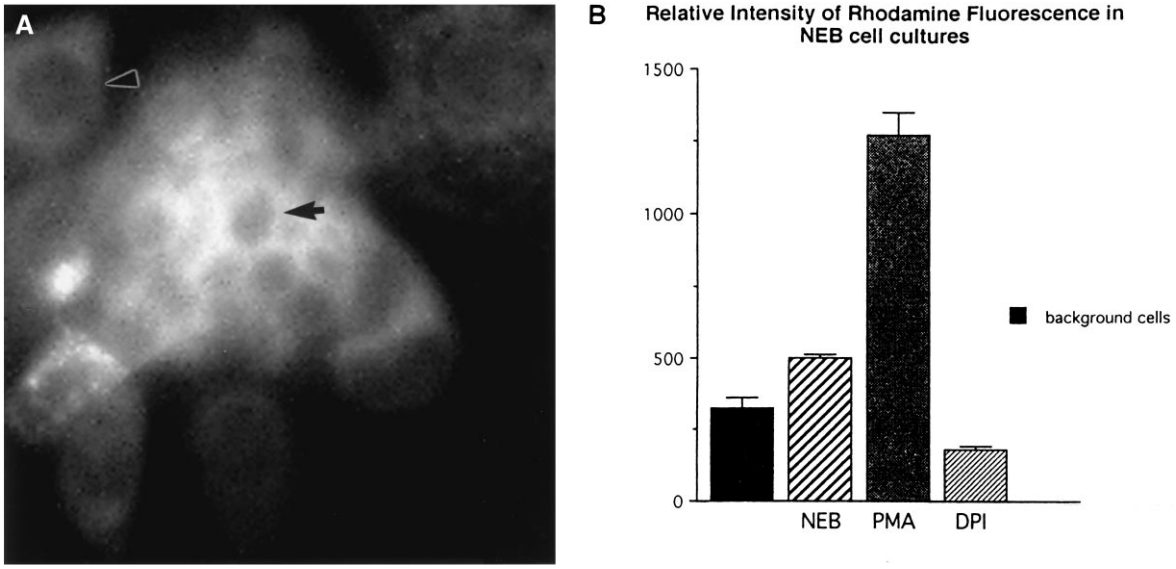

FIG. 4. Fluorescence assay for H_2O_2 generation using DHR 123 as a probe. (*A*) Unstimulated culture of rabbit fetal NEB cells 20 min after loading with DHR 123 shows fluorescence of NEB cell cytoplasm. Small, tightly packed nuclei of NEB cells (arrow) contrast with large nuclei of background lung cells (arrowhead) with dark nonfluorescent cytoplasm. (×1000.) (*B*) Relative intensity of rhodamine fluorescence in NEB cell cultures. Mean values for all background cells ($n = 8$) from different experiments. Baseline values for unstimulated NEB ($n = 8$) is significantly greater than background cells. Following a 20-min incubation with PMA, there is up to three-fold increase in fluorescence intensity indicating upregulation of the oxidase. A similar incubation with DPI ($n = 4$) resulted in marked decrease in fluorescence intensity indicating inhibition of oxidase activity.

subunits of the NADPH oxidase was identified in the same NEB cell clusters. Northern blot analysis indicated that the mRNAs of $gp91^{phox}$ subunit of the oxidase and KV3.3a transcripts in NEB cells of fetal rabbit and neonatal human lung matched in size those reported in other tissues (16, 18).

The KV3.3a channel subunit expressed in *Xenopus* oocytes generates a slowly inactivating K^+ current that is blocked by tetraethylammonium (13, 14). Whole cell K^+ currents of cultured fetal rabbit NEB cells revealed a slowly inactivating K^+ current similar to the one described in *Xenopus* oocytes expressing KV3.3a channel subunit (13). The KV3.3a channel subunit expressed in the oocyte model was insensitive to changes in pO_2, but sensitive to H_2O_2. We have shown (3) that the K^+ current recorded form fetal rabbit NEB cell cultures was decreased by exposure to reduced pO_2 suggesting a possible link between the O_2-binding protein (NADPH oxidase) and the O_2-sensitive K^+ channel. Here we report that the K^+ current recorded from fetal rabbit NEB cell cultures was increased by exposure to H_2O_2 indicating that the KH_2O_2channel on NEB cell membranes can be regulated by reactive oxygen intermediates produced by the oxidase.

A potential candidate for an oxygen sensor protein is the heme-linked NADPH oxidase, a membrane associated enzyme complex that can generate high concentrations of superoxide, the precursor to H_2O_2, as occurs in granulocytes and macrophages (9, 10). The $p91^{phox}$ polypeptide of the NADPH oxidase as well as other components of this complex have been demonstrated immunocytochemically in cultured fetal rabbit

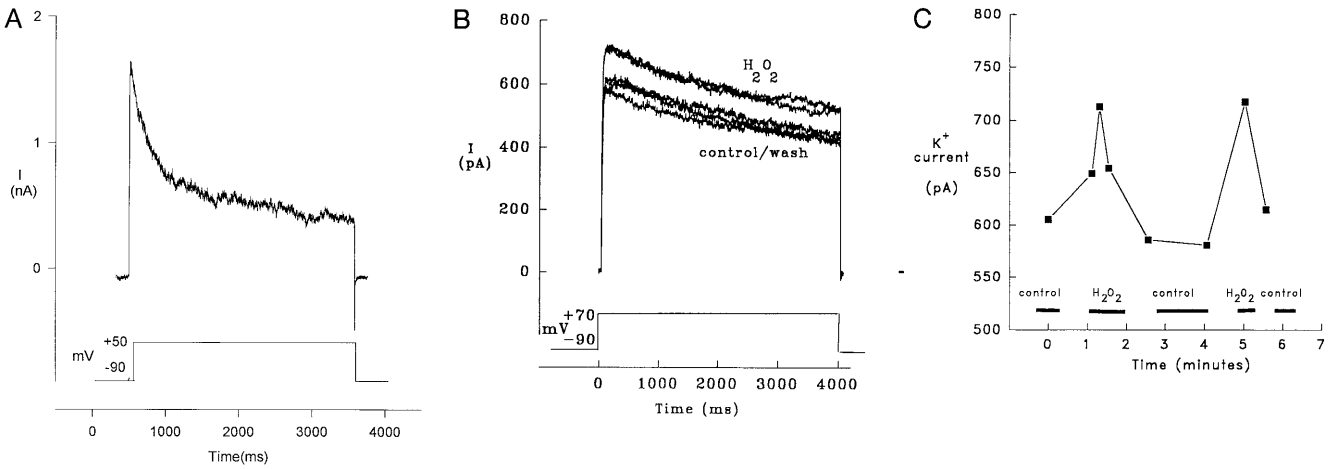

FIG. 5. Whole-cell currents in cultured fetal rabbit NEB cells. When NEB cells were exposed to a brief period of hyperpolarization followed by a longer depolarizing pulse, a slowly inactivating I_A current was revealed ($n = 15$). (*A*) NEB cells shown was recorded in the presence of an extracellular bathing solution A and an intracellular pipette solution containing: 140 mM KCl, 1 mM $CaCl_2$, 10 mM EGTA, and 10 mM Hepes. NEB cells were stepped from −90 mV to various depolarizing potentials for 3–4 sec ($n = 8$). The addition of 2 mM MgATP in the pipette solution did not alter the results. The slowly inactivating K^+ current observed was similar to the one described in *Xenopus* oocytes KV3.3a channel subunit expressing cells (13). (*B*) An increase in the K^+ current was observed when NEB cells were exposed to either brief or prolonged depolarizing pulses in the presence of varying concentrations of H_2O_2 ($n = 3$). The trace shown is of a NEB cell stepped from −90 mV to +70 mV for 4 sec in the presence of extracellular solution B. This solution was used to eliminate any contribution of Ca^{2+} and Na^+ currents. There was a resultant increase in the K^+ current in the presence of H_2O_2 (0.1–1.6 mM) that was reversible upon returning the cell to H_2O_2-free solution. This effect was repeated two times on the cell shown. (*C*) A graph depicting the change in maximal amplitude of the K^+ current over time of the same cell as in *B*.

NEB (3, 6). In contrast to granulocytes and macrophages, which depend on prior stimulation to generate oxidase activity (9, 10, 12), the oxidase appear to be active even in the basal state in NEB cells (Fig. 4 *A* and *B*).

These findings, together with the present evidence, provide a possible model for chemoreception in NEB (Fig. 6). Based on supporting evidence from this study the model suggests that the NADPH oxidase is coupled to KV3.3a channel subunit and that H_2O_2 mediates the cellular response by a mechanism similar to that suggested for the chemotransduction by carotid body glomus cells (4, 5). The gating mechanism of H_2O_2 sensitive K^+ channel is postulated to involve the redox status of a cysteine residue (23). The critical cysteine is present in the alpha subunit close to the N terminus of the KV3.3 protein (as well as KV1.4 and KV 3.4) and is involved in a "ball and chain" mechanism occluding the internal mouth of the ion channel (Fig. 6) (14, 24, 25).

The physiological role of NEB as pulmonary chemoreceptors remains unknown. The prominence of NEB during the perinatal period indicates that they may be important during the transition from fetal to neonatal life (2, 26). In early postnatal life, dysfunction of NEB may be important in the pathophysiology of sudden infant death syndrome, where hyperplasia of NEB has been previously documented (21). At the NEB cell membrane level, the effects of reactive oxygen intermediates generated locally by inflammatory cells recruited in response to mild respiratory infection may interfere with the O_2-sensing mechanism (i.e., KH_2O_2) and disable the airway sensor. Such mechanism could also explain the role of mild respiratory infection as a triggering factor for sudden infant death syndrome (27).

In the adult, SCLC express neuroendocrine features similar to normal NEB cells including the presence of bioactive amine and peptide neuromodulators (28, 29). Furthermore, in the nitrosamine-induced hamster model of SCLC, neoplastic transformation is oxygen-dependent (30). We tested six different cell lines of SCLC by Northern blot analysis and found that the NADPH oxidase subunit gp91^{phox} and KV3.3a messenger RNAs were transcribed in most of the cell lines (only

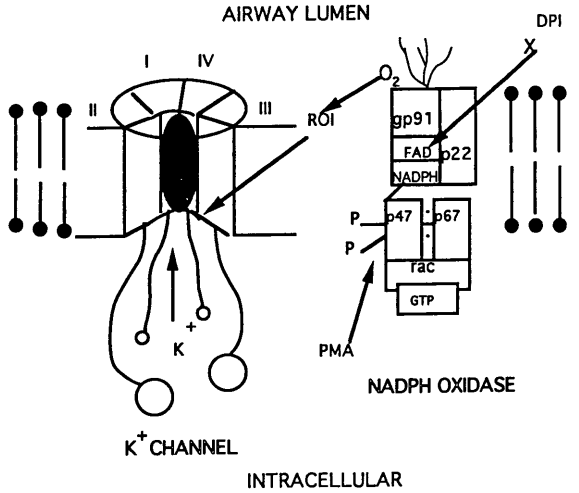

FIG. 6. In this simplified model, the NADPH oxidase complex [modified from Segal and Nugent (35)] is shown to associate with the specific K^+ channel protein. In one scenario, signaling of the ion channel response may be mediated via reactive oxygen intermediates (ROI) generated by the oxidase. Another scenario may involve signaling via metabolites at the cytoplasmic aspects of the complex (e.g., reductive events). We also indicate that DPI can inhibit oxidase function through inhibition of the flavoprotein activity while PMA can stimulate phosphorylation (i.e., activation) of the cytoplasmic components of the oxidase complex. Our immunohistochemical and electrophysiological data support functional cooperation between the oxidase and the K^+ channel during O_2 sensing.

H-128 showed weaker signals). These data further support the contention that SCLC cells are related to NEB cells (28, 29). One reason for overall lower expression of gp91^{phox} and KV3.3a in whole lung extract compared with SCLC cell lines is likely due to the sparse distribution of NEB that represent $<1\%$ of the total lung cell population (26). The contribution of other lung cell types (i.e., resident macrophages) to the overall oxidase mRNA signal is not known. However, *in situ* hybridization showed no significant signal in these other cells, indicating that their contribution is likely to be minimal. Since NEB in lung tissue are sparsely distributed and not easily accessible, SCLC cell lines expressing partial or full O_2 sensor complexes may serve as a useful model to define further the cellular and molecular mechanism of O_2 sensing. Of particular interest is the SCLC cell line H-146, in which a slowly inactivating I_A (similar to the one shown here in native NEB cells) has been previously demonstrated (31).

Homology between K^+ channels and their associated β subunits exist in both plants and bacteria such as *Escherichia coli* (32, 33). Furthermore, K^+ channels in *E. coli* have been found to be modulated by redox potential (34) suggesting a biochemical link conserved through phylogeny. Our observations thus provide a unique example of how a mammalian chemoreceptor function in the lung may operate through a biochemical mechanism well conserved during evolution but modified appropriately for diverse physiological functions.

We would like to thank Dr. G. Downey and Dr. T. Waddell for allowing us to use their equipment and for advice with the DHR assay. This work was supported in part by grants from Medical Research Council of Canada (MT 12742 and Lung Development Group to E.C. and H.Y.) and SIDS Alliance USA (to E.C.). C.Y. was recipient of Young Investigator Award from Society for Pediatric Pathology. B.R. was the recipient of National institutes of Health Grant NS30989 and Grant-in-Aid from the American Heart Association.

1. Lauweryns, J. M. & Cokeleare, M. (1973) *Z. Zellforsch. Mikrosk. Anat.* **145,** 521–540.
2. Cho, T., Chan, W. & Cutz, E. (1989) *Cell Tissue Res.* **255,** 353–360.
3. Youngson, C., Nurse, C., Yeger, H. & Cutz, E. (1989) *Nature (London)* **365,** 153–155.
4. Lopez-Barneo, J., Benot, A. R. & Urena, J. (1993) *News Physiol. Sci.* **8,** 191–195.
5. Lopez-Barneo, J. (1994) *Trend Neurosci.* **17,** 133–134.
6. Youngson, C., Nurse, C., Yeger, H., Vollmer, C., Curnutte, J. T. & Cutz, E. (1996) *Microsc. Res. Tech*., in press.
7. Lauweryns, J. M., Cokelaere, M., Deleersnyder, M. & Leibens, M. (1977) *Cell Tissue Res.* **182,** 425–440.
8. Cutz, E., Speirs, V., Yeger, H., Newman, C., Wang, D. & Perrin, D. (1993) *Anat. Rec.* **182**, 41–52.
9. Parkos, C. A., Allen, R. A., Cochrane, C. G. & Jesiatis, A. J. (1988) *Biochim. Biophys. Acta* **932**, 71–83.
10. Cross, A. R. & Jones, O. T. G. (1991) *Biochim. Biophys. Acta* **1057,** 281–298.
11. Dinauer, M. (1993) *Crit. Rev. Clin. Lab. Sci.* **30,** 329–369.
12. Babior, B. M. (1992) *Adv. Enzymol. Relat. Areas Mol. Biol.* **65,** 45–95.
13. Vega-Saenz de Miera, E. & Rudy, B. (1992) *Biochem. Biophys. Res. Commun.* **186,** 1681–1687.
14. Vega-Saenz de Miera, E., Weiser, C., Kartros, C., Lau, D., Moreno, H., Serodio, P. & Rudy B. (1994) in *Handbook of Membrane Channels,* ed. Peracchia, C. (Academic, New York), pp. 41–78.
15. Chomczynski, P. & Sacchi, N. (1987) *Anal. Biochem.* **162,** 156–159.
16. Dinauer, M. C., Pierce, E. A., Bruns, G. A. P., Curnutte, J. T. & Orkin, S. H. J. (1990) *Clin. Invest.* **86,** 1729–1737.
17. Speirs, V., Eich-Bender, S., Youngson, C. & Cutz, E. (1993) *J. Histochem. Cytochem.* **41,** 1303–1310.
18. Weiser, M., Vega-Saenz de Miera, E., Kentros, C., Moreno, H., Franzen, L., Hillman, D., Baker, H. & Rudy, B. (1994) *J. Neurosci.* **14,** 949–972.
19. Wang, D. & Cutz, E. (1994) *Lab. Invest.* **70,** 775–780.
20. Maniatis, T. M, Fritsch, E. F. & Sambrook, J. (1989) *Molecular Cloning: A Laboratory Manual* (Cold Spring Harbor Lab. Press, Plainview, NY), 2nd Ed., pp. 7.37–7.39.
21. Perrin, D. G., McDonald, T. J. & Cutz, E. (1991) *Pediatr. Pathol.* **11**, 431–447.
22. Cross, A. R. L., Henderson, L., Jones, O., Delpanio, M., Hentschel, J. & Acker, H. (1990) *Biochem. J.* **272,** 743–747.
23. Ruppersberg J., Stocker M., Pougs O., Heinemann S., Frank, R. & Koenen M. (1991) *Nature (London)* **352,** 711–714.
24. Rettig, J., Heinemann, S., Wunder, F., Lorra, C., Parcy, D., Dolly J & Pougs, O. (1994) *Nature (London)* **369,** 289–294.
25. Vega-Saenz de Miera, E., Moreus, H. & Rudy, B. (1994) *Soc. Neurosci. Abstr.* **20,** 725.
26. Cutz E., Gillan, J. & Track N. (1984) in *The Endocrine Lung in Health and Disease,* eds. Becker, K. L. & Gazdar, A. F. (Saunders, Philadelphia), pp. 210–231.
27. Howat, W. Y., Moore, E. E., Judd, M. & Roche, W. R. (1994) *Lancet* **343,** 1390–1392.
28. Gazdar, A. F., Helman, L. J., Israel, M. A., Russell, E. K., Linnoila, R. I., Mulshine, J. L., Schuller, H. M. & Park, J. G. (1988) *Cancer Res.* **48,** 4078–4082.
29. Moody, T. W., Pert, C. B., Gazdar, A. F., Carney, D. N. & Minna, J. D. (1981) *Science* **214,** 1246–1248.
30. Schuller, H. M. (1991) *Exp. Lung Res.* **17,** 837–852.
31. Pancrazio, J. J., Viglione, M. P., Tabbara, I. A. & Kim, Y. I. (1988) *Cancer Res.* **49,** 71–83.
32. McCormack, T. & McCormack, K. (1994) *Cell* **79,** 1133–1135.
33. Milkman, R. (1994) *Proc. Natl. Acad. Sci. USA* **91,** 3510–3514.
34. Meury, J. & Rubin, A. (1990) *Arch. Microbiol.* **154,** 475–482.
35. Segal, A. W. & Nugent, H. A. (1992) in *Biological Oxidants: Generation and Injurious Consequences,* eds. Chochrane, C. C & Gimbrone, M. A. (Academic, San Diego), pp. 1–20.